CELL STRUCTURE AND FUNCTION 40: 1–12 (2015)

In vivo Screening for Substrates of Protein Kinase A Using a Combination of Proteomic Approaches and Pharmacological Modulation of Kinase Activity

Tomonari Hamaguchi, Shinichi Nakamuta, Yasuhiro Funahashi, Tetsuya Takano, Tomoki Nishioka, Md. Hasanuzzaman Shohag, Yoshimitsu Yura, Kozo Kaibuchi, and Mutsuki Amano*

[1]*Department of Cell Pharmacology, Nagoya University, Graduate School of Medicine, 65 Tsurumai, Showa, Nagoya 466-8550, Japan*

ABSTRACT. **Protein kinase A (PKA) is a serine/threonine kinase whose activity depends on the levels of cyclic AMP (cAMP). PKA plays essential roles in numerous cell types such as myocytes and neurons. Numerous substrate screens have been attempted to clarify the entire scope of the PKA signaling cascade, but it is still underway. Here, we performed a comprehensive screen that consisted of immunoprecipitation and mass spectrometry, with a focus on the identification of PKA substrates. The lysate of HeLa cells treated with Forskolin (FSK)/3-isobutyl methyl xanthine (IBMX) and/or H-89 was subjected to immunoprecipitation using anti-phospho-PKA substrate antibody. The identity of the phosophoproteins and phosphorylation sites in the precipitants was determined using liquid chromatography tandem mass spectrometry (LC/MS/MS). We obtained 112 proteins as candidate substrates and 65 candidate sites overall. Among the candidate substrates, Rho-kinase/ROCK2 was confirmed to be a novel substrate of PKA both *in vitro* and *in vivo*. In addition to Rho-kinase, we found more than a hundred of novel candidate substrates of PKA using this screen, and these discoveries provide us with new insights into PKA signaling.**

Key words: Protein kinase A, Mass spectrometry, Phosphorylation, Rho-kinase

Introduction

Protein kinase A (PKA) is one of the first discovered kinases, and has been a central model for the study of signal transduction (Walsh *et al.*, 1968; Walsh and Van Patten, 1994). PKA is serine/threonine kinase activated in accordance with the cellular concentration of cAMP (Granot *et al.*, 1980). The PKA pathway begins extracellularly with an interaction between a ligand and its respective G protein coupled receptor (GPCR). When an external signaling molecule, such as adrenaline or dopamine, binds to a GPCR, the GPCR undergoes a conformational change (Ghanouni *et al.*, 2001). The Gs protein is activated by an active-state GPCR, which then activates adenylyl cyclase to increase the synthesis of cAMP (Pohl *et al.*, 1971; Tesmer *et al.*, 1997). This signaling cascade results in the activation of PKA, which in turns regulates a wide variety of physiological functions, such as contraction of the heart (Le Peuch *et al.*, 1979), during emotional behaviors (Self *et al.*, 1998) through the phosphorylation of various substrates including calcium channels and CREB (Holz *et al.*, 1986; Yamamoto *et al.*, 1988; Gonzalez and Montminy, 1989). Inactive PKA is a heterotetramer composed of a catalytic subunit dimer and a regulatory subunit dimer. The binding of cAMP to the regulatory subunit promotes a dissociation into a dimer of regulatory subunits and two active monomeric catalytic subunits (Granot *et al.*, 1980). The consensus phosphorylation motif of PKA is arginine-arginine-X-serine, where X is a hydrophobic amino acid (Kemp *et al.*, 1975, 1977). Although much is known regarding the downstream targets of PKA, there remains unidentified targets that could explain more of the physiological functions in which PKA participates. To expand on the knowledge surrounding PKA signaling, phosphoproteomics presents an ideal method for investigation.

*To whom correspondence should be addressed: Mutsuki Amano, Department of Cell Pharmacology, Nagoya University, Graduate School of Medicine, 65 Tsurumai, Showa, Nagoya 466-8550, Japan.
Tel: +81–52–744–2075, Fax: +81–52–744–2083
E-mail: m-amano@med.nagoya-u.ac.jp

Abbreviations: aa, amino acids; Ab, antibody; cAMP, cyclic AMP; DMSO, dimethyl sulfoxide; FBS, fetal bovine serum; FSK, Forskolin; GPCR, G protein coupling receptor; IB, immunoblot; IBMX, 3-isobutyl-1-methylanxthine; IP, immunoprecipitation; LC/MS/MS, Liquid Chromatography tandem Mass Spectrometry; MLC, myosin light chain; MYPT1, myosin phosphatase-targeting subunit 1; RB, Rho-binding; PCR, polymerase chain reaction; PH, pleckstrin homology; PKA, protein kinase A; RhoK, Rho-kinase; WT, wild type.

Mass spectrometry has technically advanced to a point at which phosphorylation dynamics can be elucidated (Mann *et al.*, 2002). Advances not only in instrumental development but also in the sample preparation technique prior to the ionization have contributed to the enhanced sensitivity and specificity. Among several approaches, the development of antibodies that can recognize and immunoprecipitate phosphorylated substrates specifically is a good example of improvements made in the investigation of downstream signaling (Moritz *et al.*, 2010).

We report here a comprehensive phosphoproteomic approach for PKA substrate screening using FSK and IBMX, as well as the PKA inhibitor, H-89. The lysates of HeLa cells treated with FSK and IBMX and/or H-89 were subjected to immunoprecipitation using anti-phospho-PKA substrate Ab to enrich for phosphoproteins. The identity of the phosophoproteins and phosphorylation sites in the precipitants was determined by liquid chromatography tandem mass spectrometry (LC/MS/MS). We obtained 112 proteins as candidate substrates, including Rho-kinase, and 65 candidate sites overall.

Materials and Methods

Reagents and chemicals

The following antibodies and chemicals were purchased from commercial sources: GST-PKA-cat (Carna Biosciences, Kobe, Japan); anti-VASP antibody, anti-phospho-VASP (serine 157) antibody, rabbit monoclonal anti-phospho-PKA substrate (RRXS*/T*) (100G7E) antibody, rabbit monoclonal anti-phospho-Akt substrate (RXXS*/T*) (110B7E) antibody (Cell Signaling Technology, Danvers, MA, US); anti-GSK-3β antibody (BD Biosciences, San Jose, CA, US); anti-phospho-GSK-3β (serine 9) (R&D Systems, Minneapolis, MN, US); mouse monoclonal anti-Rho-kinase antibody (ab56661) (Abcam, Cambridge, MA, US); goat polyclonal anti-Rho-kinase antibody (C-20) (Santa Cruz Biotechnology, Dallas, TX, US); Alexa-555-conjugated secondary antibodies against rabbit IgG, Alexa-647-conjugated secondary antibodies against mouse IgG, CellTracker™ Violet BMQC Dye and SYTO 16 green fluorescent nucleic acid stain (Life Technologies, Carlsbad, CA, US); [γ-^{32}P]ATP (PerkinElmer, Waltham, MA, US); Forskolin (FSK), 3-Isobutyl-1-methylanxthine (IBMX) and H-89 (Merck Millipore, Billerica, MA, US); and trypsin for mass spectrometry (Promega Co, Madison, WI, US). Rabbit polyclonal antibody against Rho-kinase phosphorylated at serine 1379 was produced against the phosphopeptide, CSIRRPpSRQLAP.

Plasmid construction

Rho-kinase-coil (421–1137 aa), Rho-kinase-RB/PH, Rho-kinase-RB/PH(TT) (941–1388 aa where asparagine 1036 and lysine 1037 were replaced by threonines to abolish the Rho binding ability), Rho-kinase-PH (1125–1388 aa), Rho-kinase-PH (1125–1237 aa), Rho-kinase-PH (1125–1337 aa), Rho-kinase-PH (1152–1388 aa) and Rho-kinase-PH (1261–1388 aa) were amplified using polymerase chain reaction (PCR) and subcloned into the pEGFP-C1 (Takara Bio, Shiga, Japan) plasmid vector. Rho-kinase-cat KD (6–553 aa lysine 121, which is essential for ATP-binding, is replaced by glycine), Rho-kinase-coil (421–701 aa) and Rho-kinase-RB/PH(TT) were amplified using PCR and subcloned into pGEX-2T (GE Healthcare, Piscataway, NJ, US) or pMal-C2 (New England Biolabs, Ipswich, MA). GST-fusion and MBP-fusion proteins were produced in *E. coli* and purified on Glutathione Sepharose 4B (GE Healthcare) and amylose resin (New England Biolabs), respectively. The cDNAs of Rho-kinase-RB/PH-1342A, Rho-kinase-RB/PH-1361A, Rho-kinase-RB/PH-1362A, Rho-kinase-RB/PH-1365A, Rho-kinase-RB/PH-1366A, Rho-kinase-RB/PH-1374A, and Rho-kinase-RB/PH-1379A in which an alanine is substituted for the corresponding serine, were generated via site-directed mutagenesis and subcloned into the pEGFP-C1 plasmid.

Cell culture and Immunoblot analysis

COS-7 and HeLa cells were cultured in Dulbecco's modified Eagle's medium (DMEM, Sigma-Aldrich, St. Louis, MO, US) with 10% FBS. All cell lines were grown in a humidified atmosphere of 5% CO_2 at 37°C. Transfection was performed using the Lipofectamine 2000 reagent (Life Technologies) according to the manufacturer's instructions. Cells were grown over night. Cells were treated with dimethyl sulfoxide (DMSO) or H-89 for 30 min, and then treated with or without a Forskolin and IBMX mixture for 30 min without replacing the medium. The cells were lysed with SDS sample buffer and subjected to SDS-PAGE and immunoblot analysis with the indicated antibodies.

Immunoprecipitation

HeLa cells were seeded in a 100 mm dish at a density of 1.0×10^6 in DMEM with 10% FBS and cultured overnight at 37°C. Cells were treated with FSK, IBMX and/or H-89 as described above. The cells were gently washed with ice-cold PBS and scraped off the plate with ice-cold lysis buffer (20 mM Tris/HCl, pH 7.5, 1% NP-40, 1 mM EDTA, 1 mM dithiothreitol, 150 mM NaCl, 80 mM β-glycerolphosphate, 80 mM NaF, 4 μg/ml Leupeptin, 0.1 μM (p-Amidinophenyl) methanesulfonyl fluoride, 1 μg/ml aprotinin, 50 nM Calyculin A). The lysate was incubated for 30 min at 4°C with rotation and centrifuged at 17,000×g for 20 min at 4°C; the supernatant was used as the cell lysate. The indicated antibodies were incubated with the lysate for 1 hour at 4°C with rotation and then immobilized on Protein A Sepharose 4 Fast Flow beads (GE Healthcare) with rotation for 1 hour. The beads were then washed with lysis buffer twice and then with wash buffer (20 mM Tris/HCl, pH 7.5, 1 mM EDTA, 1 mM dithiothreitol, 150 mM NaCl) three times.

LC/MS/MS

The method of sample preparation for mass spectrometry was per-

formed as previously described (Nishioka *et al.*, 2012). Briefly, after the immunoprecipitation with anti-phospho-PKA substrate Ab was performed, the bound proteins were extracted from the beads with a guanidine solution (50 mM Tris/HCl, 7 M guanidine), and the eluate was subjected to reduction, alkylation, demineralization, concentration and then digestion with trypsin. One fourth of the digest was passed through a SPE C-TIP (Nikkyo Technos, Tokyo, Japan) and introduced to LC/MS/MS for total peptide analysis, and the remaining sample was passed through a Titansphere® Phos-TiO Kit (GL Sciences, Tokyo, Japan) and SPE C-TIP for an enriched phosphopeptide analysis. LC/MS/MS was performed using the Q-Exactive mass spectrometry (Thermo-Fisher Scientific Inc., Waltham, MA) system combined with an HTC-PAL autosampler and the Michrom nano-Advance UHPLC (Michrom BioResources Inc., CA) with a MonoCap C18 Nano-flow (0.1×150 mm) column (GL Science, Tokyo, Japan) and the Michrom's ADCANCE CaptiveSpray Ionization Source. A peak list was generated and calibrated using MaxQuant software (version 1.2.2.5) (Cox and Mann, 2008). Database searches were performed against the complete proteome set of *Homo sapiens* in UniProtKB 2013_07 and concatenated with reversed copies of all the sequences (Peng *et al.*, 2003). False discovery rates (FDRs) for the peptide, protein and site levels were set to 0.01. When the identified peptides satisfied the following criteria, they were regarded to be candidate substrates; the ion intensity of the identified peptides in the HeLa lysate treated with FSK/IBMX was more than twice as high as those in the lysate treated with other drug combinations; the ion intensity of the identified peptides decreased in accordance with the concentration of H-89. Phosphopeptide identifications with a localization probability of ≥0.75 were accepted.

Phosphorylation assay

The phosphorylation assay was performed as previously described (Amano *et al.*, 1996b). The kinase reactions tested the activity of PKA on GST-fusion proteins (1 μM) and MBP-fusion proteins (1 μM) produced in *E. coli* and GFP-fusion proteins obtained from COS-7 cells. The reactions (50 μl total volume) consisted of a reaction mixture (50 mM Tris/HCl, pH 7.5, 1 mM EDTA, 1 mM EGTA, 1 mM dithiothreitol, 5 mM MgCl2, 100 μM [γ-^{32}P] ATP [1 to 20 GBq/mmol]), 0.02 μM purified GST-PKA-cat and substrates and was carried out for 30 min at 30°C. The reaction mixtures were then boiled in SDS sample buffer and subjected to SDS-PAGE. The radiolabeled proteins were analyzed using an image analyzer, Typhoon FLA 9000 (GE healthcare).

Cortical neuron culture

Cortical neurons were prepared from E16 ICR mouse embryos using papain as described previously (Goslin and Banker, 1989; Inagaki *et al.*, 2001). Briefly, neurons were seeded on dishes coated with poly-D-lysine and cultured for 72 h in neurobasal medium (Life Technologies) supplemented with B-27 (Life Technologies) and 1 mM GlutaMAX (Life Technologies). Neurons were treated with DMSO or 10 μM H89 for 30 min and then with or without 10 μM Forskolin and 50 μM IBMX for 30 min. The cell lysates were analyzed using immunoblot analysis with the indicated antibodies.

Preparation and incubation of striatal slices

Striatal slices were prepared from mice as described previously (Nishi *et al.*, 1997). Male C57BL/6 mice at 6–8 weeks of age were decapitated. The brains were removed rapidly and placed in ice-cold, oxygenated Krebs-HCO_3^- buffer (124 mM NaCl, 4 mM KCl, 26 mM $NaHCO_3$, 1.5 mM $CaCl_2$, 1.25 mM KH_2PO_4, 1.5 mM $MgSO_4$, and 10 mM D-glucose, pH 7.4). Coronal slices (350 μm) were prepared using a vibratome, VT1200S (Leica Microsystems, Nussloch, Germany). The striatum was dissected from the slices in ice-cold Krebs-HCO_3^- buffer. Each slice was placed in a polypropylene incubation tube with 2 ml of fresh Krebs-HCO_3^- buffer containing adenosine deaminase (10 μg/ml). The slices were pre-incubated at 30°C under constant oxygenation with 95% O_2/5% CO_2 for 60 min. The buffer was replaced with fresh Krebs-HCO_3-buffer after the 30 min of pre-incubation. Adenosine deaminase was included during the first 30 min of the pre-incubation. Slices were treated with or without 100 μM dopamine (Sigma-Aldrich) for 4 min. After the drug treatment, slices were transferred to Eppendorf tubes, frozen on dry ice, and stored at –80°C until further analysis. Prior to the immunoblot analysis, the slices were mixed with SDS sample buffer and boiled.

Cell culture and immunostaining

HeLa cells were seeded on 13-mm glass coverslips coated with poly-D-lysine in a 24-well plate at a density of 1.0×10^5 in DMEM with 10% FBS and cultured overnight at 37°C. Cells were treated with FSK/IBMX and/or H-89 as described above. SYTO 16 was treated according to the manufacturer's instructions. The cells were fixed with 4% paraformaldehyde for 15 min at room temperature and washed with PBS at room temperature. The cells were then incubated with the indicated antibodies overnight at 4°C. After washing, the samples were incubated with Alexa 555- and Alexa 647-conjugated secondary antibodies. Fluorescence was examined using a Zeiss LSM 780 laser scanning microscope (Carl Zeiss, Obeokochem, Germany) with a C-Apochromat 40× (NA 1.2) objective under the control of LSM software (Carl Zeiss).

Animals

All animal experiments were performed according to the guidelines of the Institute for Developmental Research. Male C57BL/6 mice and ICR mice were purchased from Japan SLC (Shizuoka, Japan).

Statistical analyses

Statistical analyses were performed with GraphPad Prism version 5.0 (GraphPad Software, La Jolla, CA, US). $P<0.05$ was considered statistically significant.

Results

Isolation of PKA substrates in HeLa cells treated with FSK/IBMX and/or H-89

A balance between cAMP levels and phosphodiesterase activity modulates the activity of PKA in cells. FSK is a known activator of adenylyl cyclase, and IBMX is a competitive non-selective phosphodiesterase inhibitor; both activate PKA. Conversely, H-89 competes with ATP for PKA binding, which results in an inhibition of PKA (Engh *et al.*, 1996). To screen for potential substrates of PKA, we optimized the conditions of FSK, IBMX and H-89 in HeLa cells. Because VASP is known to be phosphorylated by PKA at serine 157 (Butt *et al.*, 1994), we monitored its phosphorylation level. FSK alone was not enough to raise the phosphorylation level of VASP (data not shown), and so we treated HeLa cells with IBMX simultaneously. The phosphorylation of VASP was increased by this FSK and IBMX mixture, whereas this phosphorylation was prevented in an H-89 concentration-dependent manner (Fig. 1A). In contrast, the phosphorylation of GSK-3β at serine 9 was not affected under the same conditions.

Anti-phospho-PKA substrate Ab is directed against the motif RRXS*/T*, where phosphorylated serine (S*) or threonine (T*) is fixed at the 0 position and R is fixed at the –3 and –2 positions (Zhang *et al.*, 2002). Anti-phospho-PKA substrate Ab detected the increase in phosphorylation levels of many proteins in the HeLa cell lysates treated with FSK and IBMX in addition to the decrease when treated with H-89 (Fig. 1B). Anti-phospho-Akt substrate Ab did not detect either the increase in phosphorylation levels by FSK/IBMX or the decrease by H-89 (Fig. 1B). Thus, anti-phospho-PKA substrate Ab could be employed to specifically detect both the activation and inactivation of PKA signaling under our conditions.

To enrich phosphorylated proteins, the HeLa cell lysates treated with H-89 and/or FSK and IBMX mixture were subjected to immunoprecipitation using anti-phospho-PKA substrate Ab. The proteins bound to anti-phospho-PKA substrate Ab were eluted with guanidine solution, followed by immunoblot analysis with anti-phospho-PKA substrate Ab. (Fig. 2A) The signal intensity of the precipitants changed in accordance with the level of PKA activation, suggesting that anti-phospho-PKA substrate Ab enriched phosphorylated PKA substrates under these drug conditions.

LC/MS/MS analysis of phosphopeptides after immunoprecipitation

To identify the proteins bound to anti-phospho-PKA substrate Ab, these proteins were extracted and digested by trypsin. For the enriched phosphopeptide analysis, three fourths of the digest was introduced to a TiO_2 column and

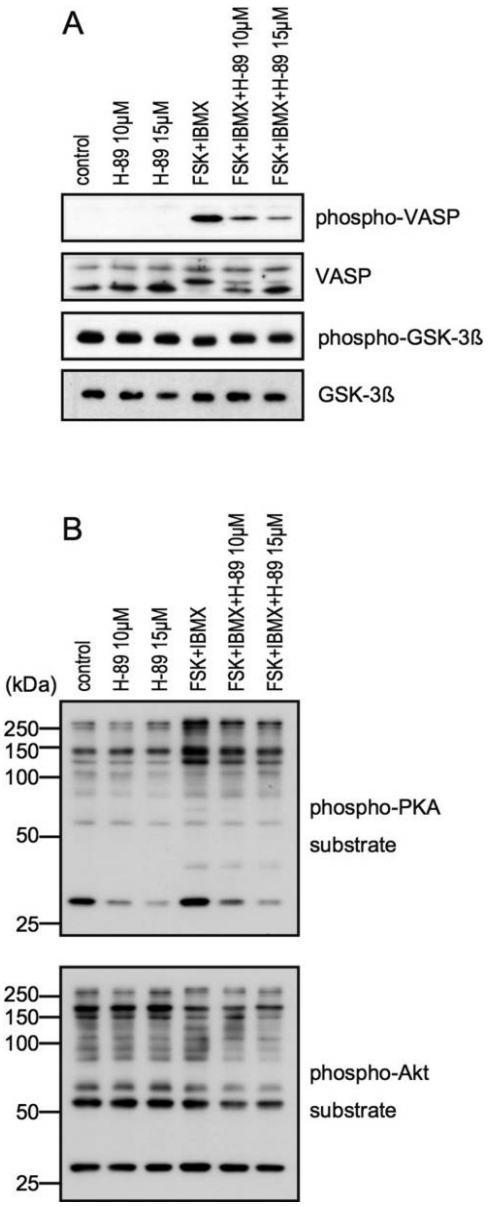

Fig. 1. Optimization of drug treatment conditions to activate or inhibit PKA signaling. (A) Immunoblot analysis of HeLa cell lysates treated with FSK/IBMX and/or H-89. HeLa cells were treated with H-89 at 10 μM or 15 μM for 30 min, followed by a treatment with an FSK and IBMX mixture for 30 min. FSK and IBMX induced VASP phosphorylation at serine 157, and H-89 inhibited this phosphorylation according to H-89 concentration. Phosphorylation of GSK-3β at serine 9 was neither induced nor inhibited significantly under the conditions. (B) Immunoblot analysis of HeLa cell lysates detected by anti-phospho-PKA substrate Ab or anti-phospho-Akt substrate Ab. Anti-phospho-PKA substrate Ab detected both an increase in phospho-signal from the lysate treated with the FSK and IBMX mixture and a decrease in the lysate signal treated with H-89 but anti-phospho-Akt substrate Ab did not.

were subsequently subjected to LC/MS/MS using a Q Exactive mass spectrometer (Fig. 2B). Using this enriched phosphopeptide analysis we identified 65 phosphorylation

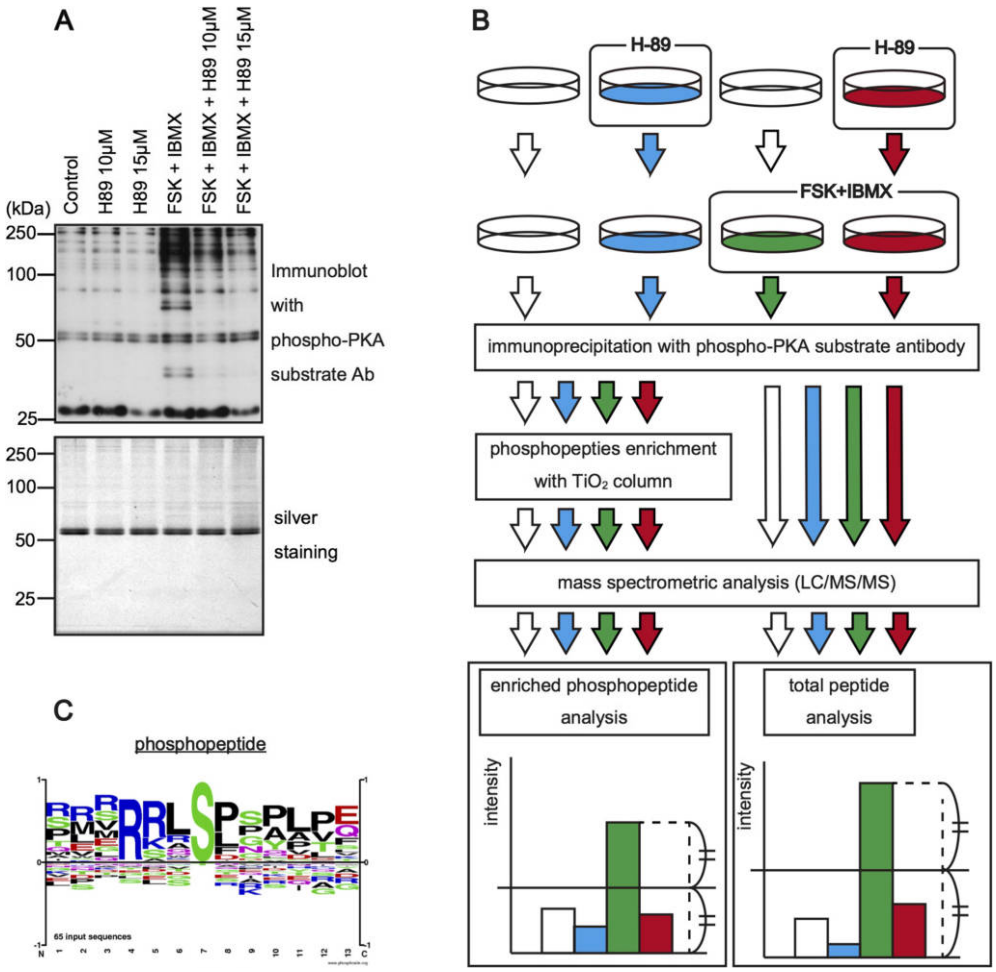

Fig. 2. Identification of PKA substrates. (A) Enrichment of proteins immunoprecipitated with anti-phospho-PKA substrate Ab. HeLa cell lysates treated with FSK/IBMX and/or H-89 were subjected to immunoprecipitation using anti-phospho-PKA substrate Ab. The bound proteins were eluted off by a guanidine solution (50 mM Tris/HCl, 7 M guanidine), followed by reduction, alkylation, demineralization and concentration. The eluate was analyzed using SDS-PAGE and visualized using both immunoblot analysis with anti-phospho-PKA substrate Ab and silver staining. (B) The strategy for identification of PKA substrates. The digest was passed through a TiO_2 column for the enriched phosphopeptide analysis but it did not for the total protein analysis. (C) The sequence alignment of phosphopeptides detected with the enriched phosphopeptide analysis.

sites derived from 46 proteins whose ion intensities in the sample treated with FSK/IBMX were more than twice as high as the others and decreased in accordance with the concentration of H-89 (Table I). Known phosphorylation sites, such as CAD (pS1859), CAMKK1 (pS458) and RAF (pS259) were detected using this analysis. As for the substrates of ARHGEF7 and EVL, the phosphorylation sites detected in this analysis were different from those that have been previously reported. The sequence alignment of the detected phosphopeptides was similar to the consensus motif of PKA (Fig. 2C).

Because the amount of proteins phosphorylated by PKA was increased by the stimulation of FSK/IBMX, the amount of precipitated protein using anti-phospho-PKA substrate Ab was also increased. Therefore, it was important to compare the intensity of total peptides without enrichment by the TiO_2 column. By total peptide analysis, we identified 81 proteins as phosphoproteins whose ion intensities in the sample treated with FSK/IBMX were more than twice as high as the others and decreased in accordance with the concentration of H-89. This study also identified several known substrates, such as ENAH, VASP and EVL (Table II). Of the identified proteins, 12 proteins were detected both by phosphopeptide analysis and total peptide analysis.

PKA phosphorylates Rho-kinase at Ser1379

After obtaining the mass spectrometry results, we focused on ROCK2/Rho-kinase (hereafter referred to as Rho-

Table I. CANDIDATE SUBSTRATES FROM THE RESULT OF ENRICHED PHOSPHOPEPTIDE ANALYSIS

Gene	UniProtKB	p-site position	Sequence Window
ACIN1	B4DQZ7	302	DRKKA**S**LVALP
ARHGEF7	Q14155-5	645	SSRKE**S**APQVL
BAT2	P48634	1147	PGAPP**S**PAPAR
C17orf59	Q96GS4	196	GGRRA**T**ISSPL
C19orf21	Q8IVT2	394	LRRAL**S**SDSIL
C2CD5	F5H5R1	260	LPACN**S**PSKEM
C2orf55	Q6NV74	244	KMRRL**S**SRAQS
C2orf55	Q6NV74	245	MRRLS**S**RAQSE
C2orf55	Q6NV74	249	SSRAQ**S**ESLSD
C2orf55	Q6NV74	251	RAQSE**S**LSDLT
C2orf55	Q6NV74	253	QSESL**S**DLTCT
CAD	P27708	1406	GGRRL**S**SFVTK
CAD	P27708	1859	RIHRA**S**DPGLP
CAMKK1	F8W9H1	496	MLRKR**S**FGNPF
CAMKK1	F8W9H1	513	EERSM**S**APGNL
CAMKK2	Q96RR4	511	EERSL**S**APGNL
CASP11	Q99590	608	EELIE**S**PKLES
CDC25B	P30305-4	396	VLRSK**S**LCHDE
CDK18	B4DK03	128	VSKRL**S**LPMDI
CEP72	Q9P209	237	SRHLL**S**PQLVQ
CRY2	B4DZD6	283	RMNAN**S**LLASP
DAPK2	Q9UIK4	299	MVRRE**S**VVNLE
DENND4C	Q5VZ89	1089	KERST**S**LSALV
EVL	Q9UI08-2	333	WERSN**S**VEKPV
GLI2	P10070	234	RKRAL**S** ISPLS
HSPC075	Q9UQ35	295	ALAGR**S**PSPAS
HSPC075	Q9UQ35	297	AGRSP**S**PASGR
HSPC075	Q9UQ35	323	TQRPS**S**PETAT
HSPC075	Q9UQ35	1014	LSGSK**S**PCPQE
HSPC075	Q9UQ35	2032	RRRSR**S**RTPLL
HSPC075	Q9UQ35	2034	RSRSRT**P**LLPR
HSPC075	Q9UQ35	2581	LKRVP**S**PTPAP
KIAA0556	O60303	691	NCRKD**S**LSQLE
KIAA1522	Q9P206-2	728	ISKDQ**S**PPPSP
KIAA1522	Q9P206-2	917	LRRAL**S**GRASP
KIAA1522	Q9P206-2	921	LSGRA**S**PVPAP
KIAA1522	Q9P206-2	1030	VARKP**S**VGVPP
KLC4	Q9NSK0-3	608	MKRAA**S**LNYLN
LIMCH1	G5EA03	1055	TVTRC**S**PTVAF
LIMCH1	G5EA03	1103	VVKPK**S**PEPEA
LIMCH1	G5EA03	1259	RRWKK**S**FQGDD
LRCH3	B4DEQ7	324	GDKRW**S**GNEPT
MARK3	P27448-7	426	KQRRY**S**DHAGF
NF1	P21359	2597	HLRKV**S**VSESN
NHSL1	Q5SYE7-2	190	ASLRR**S**LIYTD
OFD1	E9KL37	899	EERRQ**S**NLQEV
PCNX	Q96RV3	692	RARVL**S**LDSGT
PDE3A	Q14432	428	KRLRR**S**LPPGL
PDE8B	O95263	517	GLRRL**S**GNEYV
PHACTR2	O75167-4	571	LSRKL**S**LRPTV
PITPNM2	Q9BZ72	1277	ALRKG**S**FGLPG
PITPNM3	A1A5C9	907	ILRKG**S**FGLHA
RAF1	D7PBN3	672	RQRST**S**TPNVH
REPS1	Q96D71	272	EIRRQ**S**SSYDD
RPL18A	B2R4C0	71	QVFEK**S**PLRVK
RPLP2	P05387	105	EESEE**S**DDDMG
SAFB	A0AV56	604	KRSVV**S**FDKVK
SIK2	A8K5B8	587	EGRRA**S**DTSLT
SIK3	Q9Y2K2	568	PVRRF**S**DGAAS
SPECC1L	B2RMV2	887	PMQRH**S**ISGPI
TMCC1	A8K5Y3	414	SNFQS**S**PKYGS
TNKS1BP1	Q9C0C2	429	VQRRF**S**EGVLQ
TNKS1BP1	Q9C0C2	836	LGTQR**S**QEADV
TNKS1BP1	Q9C0C2	983	GTRPL**S**SGFSP
ZNF318	Q5VUA4	2101	SVRIP**S**PNILK

Red words : known phosphosites, Underlined words : those detected more than twice

Table II. CANDIDATE SUBSTRATES FROM THE RESULT OF TOTAL PEPTIDE ANALYSIS

Gene	UniProtKB
AKAP17A	Q02040
AP2M1	B4DNB9
ARHGEF7	Q14155-5
BAT2	P48634
BIRC6	Q9NR09
BOP1	A8K3R2
C17orf1	O95466-2
CAD	P27708
CAMKK1	F8W9H1
CEP170	E9PEY0
CNOT3	O75175
CTNNA1	P35221-2
DHC1	Q14204
DNAJ2	P31689
DOCK1	A8MU08
DOCK7	Q96N67
DPDE3	Q08499
ELMO2	B4DRL5
EML4	B5MBZ0
ENAH	Q8N8S7
EVL	Q9UI08-2
FAM122B	G1UD79
FBL	P22087
FHOD1	Q9Y613
FIBP	O43427
FISH	Q5TCZ1
FMR1L2	P51116
FNBP1L	Q5T0N5
HADH	E9KL44
HADHB	P55084
HDCMA18P	Q4G0J3
HECTD1	D3DS86
IGF2R	P11717
KIAA1522	Q9P206-2
KIF14	Q15058
KIF23	Q02241
KIF2C	A8K3S3
KLC4	Q9NSK0-3
KPM	Q9NRM7
LIMCH1	Q9UPQ0
LPP2	O43688-2
LPP3	O14495
LRCH3	Q96II8
LUZP1	Q86V48
MAP7D3	Q8IWC1
MYO10	Q9HD67
MZT1	Q08AG7
NAV1	Q8NEY1
NDEL1	B4DS41
OFD1	E9KL37
PDE3A	Q14432
PDE8A	O60658
PFKFB2	O60825
POB1	Q8NFH8
PTDSS1	A8KAH1
RCD1	B2RE59
RIF1	Q5UIP0
ROCK2	O75116
RPL1	Q59GY2
RPL10	Q5HY50
RPL17	P18621
RPL19	P84098
RPL22	P35268
RPL27A	P46776
RPL5	A2RUM7
RPS14	P62263
RPS3	P23396
RPS4X	B2R491
RUVBL1	B5BUB1
SHCBP1	A8K7Z9
SIK2	A8K5B8
SLC25A5	Q59EI9
SNIP1	B1AK66
SRGAP2	A2RUF3
SUFU	B2R5U4
TBC1D15	E9PH93
TBC1D15	Q8TC07
TBC1D5	C9JP52
TEM6	Q68CZ2
U2SURP	O15042
USP35	Q8NHA9
VASP	P50552

Red words : known substrates, Underlined words : those detected more than twice

kinase) because the relationship between PKA and Rho-kinase attracted our interest. Rho-kinase plays a key role in Rho signaling (Riento and Ridley, 2003; Amano *et al.*, 2010). First, we examined whether PKA directly phosphorylates Rho-kinase *in vitro*. We performed an *in vitro* phosphorylation assay using three fragments of Rho-kinase; a kinase dead form of the Rho-kinase catalytic domain (GST-Rho-kinase-cat KD), a truncated region of the coiled-coil domain (GST-Rho-kinase-coil (421–701 aa)) and MBP-Rho-kinase-RB/PH(TT) (Fig. 3A). PKA phosphorylated

the Rho-kinase RB/PH(TT) to a greater extent than the others, indicating that Rho-kinase is directly phosphorylated by PKA and that the RB/PH(TT) region contains the major site of phosphorylation (Fig. 3B).

We next made a long form of the Rho-kinase coiled-coil region containing the RB domain (GFP-Rho-kinase-RB/PH) and five fragments of the PH domain, each tagged with GFP, to narrow down the site of PKA phosphorylation. We found that Rho-kinase was phosphorylated within the 1261–1388 aa region (Fig. 3C). The GFP-Rho-kinase-coiled-coil region containing the RB domain was not phosphorylated by PKA. After scanning this region for the consensus sequence of PKA, we produced several mutant proteins including GST-Rho-kinase-RB/PH-1342A, -1361A, -1362A, -1365A, -1366A, -1375A, or -1379A, in which a serine or threonine was substituted with an alanine, and examined the phosphorylation efficiency (Fig. 3D). The phosphorylation level of GST-Rho-kinase-RB/PH-1379A was much lower than that of GST-Rho-kinase-RB/PH-WT (Fig. 3E). Serine 1366 of Rho-kinase has previously been reported as an autophosphorylation site (Chuang *et al.*, 2012). Alanine substitution for serine 1366 (Fig. 3E) as well as for other serine residues besides serine 1379 (data not shown) did not affect the phosphorylation level, indicating that serine 1379 is the major site of phosphorylation by PKA.

We produced a polyclonal antibody that specifically recognizes Rho-kinase when it is phosphorylated at serine 1379 (anti-phospho-Rho-kinase (pS1379) Ab). An immunoblot analysis revealed that anti-phospho-Rho-kinase (pS1379) Ab recognized Rho-kinase phosphorylated by PKA in a dose-dependent manner (Fig. 4A). To examine whether PKA phosphorylates Rho-kinase at serine 1379 *in vivo*, an immunoblot analysis of HeLa cell lysates treated with a PKA activator/inhibitor was performed using anti-phospho-Rho-kinase (pS1379) Ab. It was difficult to detect a signal for this phosphorylation site under basal conditions. FSK and IBMX treatment enhanced the phosphorylation of Rho-kinase in HeLa cells, but H-89 inhibited the FSK- and IBMX-induced phosphorylation in a concentration-dependent manner (Fig. 4B). These results indicate that PKA phosphorylates Rho-kinase at serine 1379 *in vivo*.

ROCK1 is an isoform of Rho-kinase, but ROCK1 and Rho-kinase do not share sequence homology within the region surrounding serine 1379 of Rho-kinase (data not shown). Nevertheless, we examined whether PKA also phosphorylates ROCK1. HeLa cell lysates treated with or without FSK/IBMX and/or H-89 were subjected to immunoprecipitation using either anti-ROCK1 Ab or anti-Rho-kinase Ab. The bound proteins were eluted with SDS sample buffer and were then subjected to SDS-PAGE and an immunoblot analysis using anti-phospho-PKA substrate Ab. Although the phospho-signal for the proteins precipitated with anti-Rho-kinase Ab correlated with PKA activation/inactivation, there was no signal detected for the proteins precipitated by anti-ROCK1 Ab (Fig. 4C). Thus, it is possible that PKA specifically phosphorylates Rho-kinase.

It was reported that Rho-kinase is abundantly expressed in the brain, especially in neurons (Nakagawa *et al.*, 1996; Iizuka *et al.*, 2012). Therefore, we also examined whether this phosphorylation occurs in neurons. Dissociated cortical neuron cultures were treated with FSK/IBMX and/or H-89 and subsequently lysed with SDS sample buffer (Fig. 4D). The immunoblot analysis of these lysates using anti-phospho-Rho-kinase (pS1379) Ab suggested that Rho-kinase was also phosphorylated by PKA in cultured neurons. Next, we examined whether this phosphorylation was induced under more physiological conditions (Fig. 4E). To this end, we treated striatum slice cultures with dopamine, a natural agonist. Dopamine increased the phosphorylation of Rho-kinase at serine 1379 in the striatum. These results indicate that dopamine stimulates PKA signaling to phosphorylate Rho-kinase in neurons.

To visualize the localization of Rho-kinase when phosphorylated at serine 1379, we performed immunostaining of HeLa cells using anti-phospho-Rho-kinase (pS1379) Ab and mouse anti-Rho-kinase Ab (Fig. 5A). Treatment with FSK and IBMX increased the intensity of phosphorylated Rho-kinase in the cytosol partly as dot-like structures, suggesting that Rho-kinase was phosphorylated mainly in this cellular compartment. Adding H-89 together with FSK and IBMX decreased this phosphorylation. The signal intensity in the cytosol was almost identical in both the control and H-89 treated cells (Fig. 5B). The phospho-signal detected in the nucleus could be non-specific under our conditions because this nuclear signal was not affected by the knockdown of Rho-kinase (data not shown). Therefore, these data suggest that phosphorylated Rho-kinase is mainly localized in the cytosol.

Discussion

In this study, we identified a large number of known PKA substrates in addition to a number of novel candidate substrates. More than half of our identified candidate substrates and phosphosites have not been previously reported. We also found that PKA phosphorylates Rho-kinase at serine 1379 both *in vitro* and *in vivo*.

We employed two analyses depending on whether the immunoprecipitants were additionally passed through a TiO_2 column: enriched phosphopeptide analysis and total peptide analysis. For enriched phosphopeptide analysis, we could detect candidate substrates whose peptide sequences were identical to the consensus motif of PKA substrates. Because certain types of phosphopeptides are difficult to detect with mass spectrometry, we also used a total peptide analysis to screen for phosphoproteins that change in total

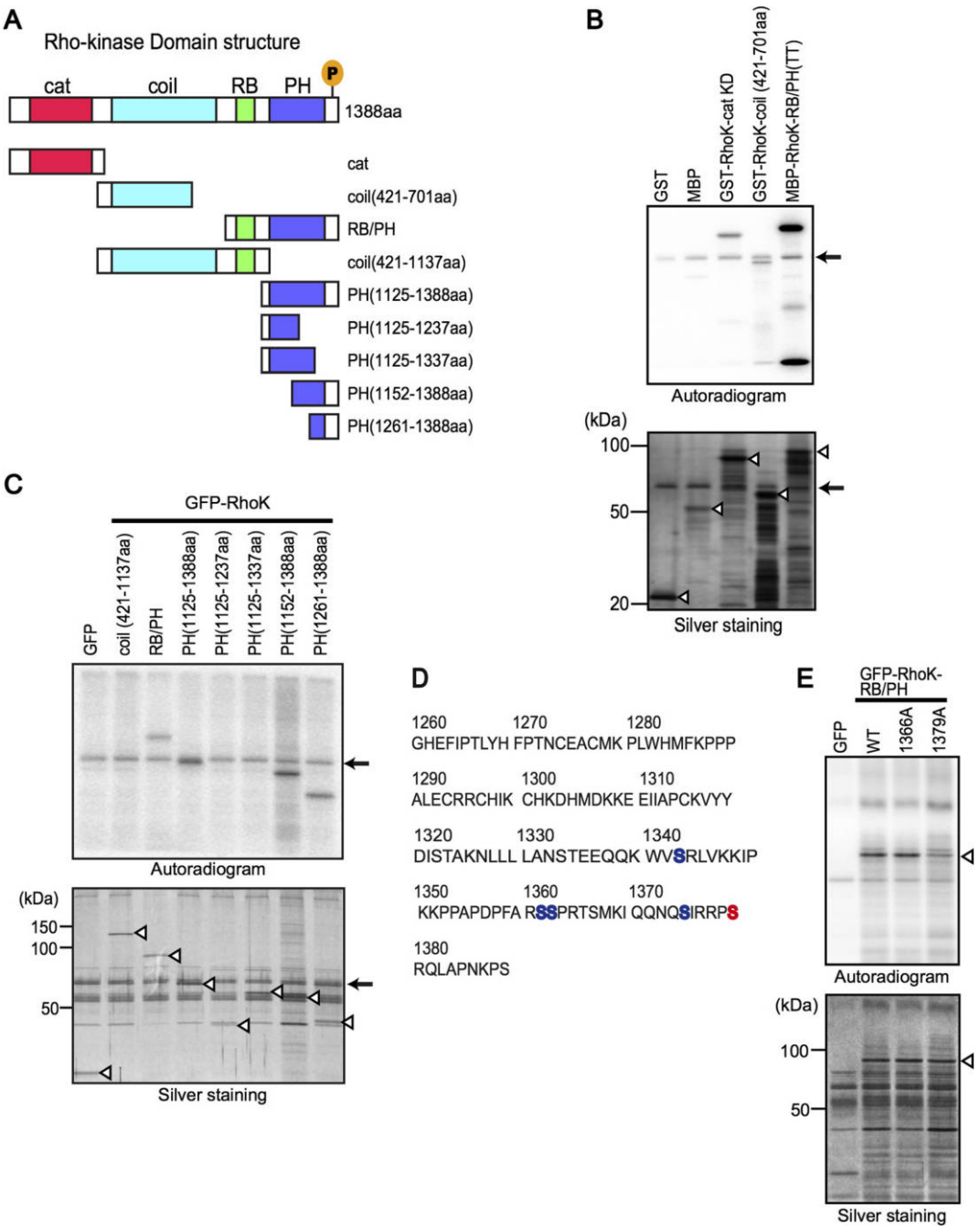

Fig. 3. Identification of a PKA phosphorylation site on Rho-kinase. (A) A schematic representation of Rho-kinase. The domain organization of Rho-kinase and its fragments are represented. "P" in an orange circle indicates the phosphorylation site. (B, C and E) Phosphorylation of Rho-kinase fragments by PKA. (B) GST-Rho-kinase-cat KD, GST-Rho-kinase-coil (421–701 aa) and MBP-Rho-kinase-RB/PH(TT) were produced and purified from E. coli. They were incubated with GST-PKA-cat and 100 μM [γ-^{32}P] ATP for 30 min at 30°C. The reaction mixtures were subjected to SDS-PAGE and GST- and MBP-fused proteins were visualized by silver staining (lower panel). Phosphorylated proteins were imaged using autoradiography (upper panel). Open arrowheads and arrows indicate the positions of the corresponding proteins and the auto phosphorylation of GST-PKA-cat, respectively. (C) Phosphorylation of immunoprecipitated Rho-kinase in COS-7 cells. GFP-Rho-kinase fragments were transiently expressed in COS-7 cells. They were subjected to immunoprecipitation with anti-GFP Ab. The precipitants were phosphorylated and subjected to SDS-PAGE. Silver staining is in the lower panel and autoradiography is in the upper panel. (D) Sequence of potential phosphorylation sites (blue) within the 1261–1388 aa region. The major phosphorylation site was identified as serine 1379 (red). (E) Phosphorylation of immunoprecipitated Rho-kinase mutants with amino acid substitutions. Transfection, immunoprecipitation and phosphorylation assays were described as above. Silver staining is in the lower panel and autoradiography is in the upper panel. Open arrowheads indicate the positions of the GFP-Rho-kinase-RB/PH and its mutants.

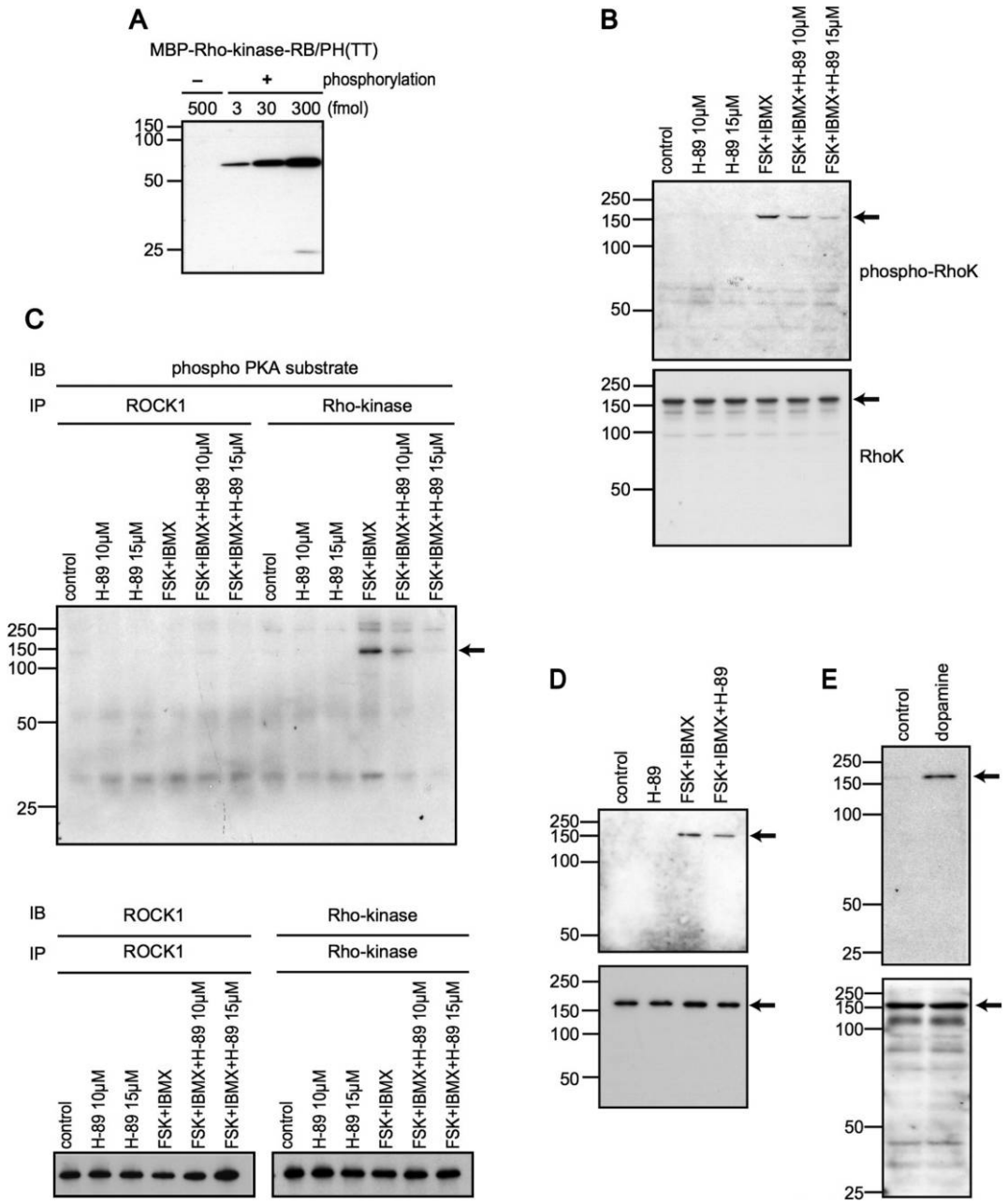

Fig. 4. Phosphorylation of Rho-kinase *in vivo*. (A) Specificity of the antibody against Rho-kinase phosphorylated at serine 1379 (anti-phospho-Rho-kinase (pS1379) Ab). MBP-Rho-kinase-RB/PH(TT) (500 fmol) containing the indicated amounts of phosphorylated MBP-Rho-kinase-RB/PH(TT) was subjected to SDS-PAGE, followed by immunoblot analysis with anti-phospho-Rho-kinase (pS1379) Ab. (B) Phosphorylation of Rho-kinase in HeLa cells. The HeLa cell lysates were analyzed using immunoblot analysis with anti-phospho-Rho-kinase (pS1379) Ab (upper panel) and mouse anti-Rho-kinase Ab (lower panel). Arrows indicate the positions of the corresponding proteins. (C) Immunoblot analysis of immunoprecipitated ROCK1 or Rho-kinase using anti-phospho-PKA substrate Ab. HeLa cells were treated with FSK, IBMX and/or H-89 as indicated. They were subjected to immunoprecipitation with anti-ROCK1 Ab or goat anti-Rho-kinase Ab. Immunoblot analysis was performed with these precipitants and detected with anti-phospho-PKA substrate Ab (upper panel), anti-ROCK1 Ab, or mouse anti-Rho-kinase Ab (lower panel). (D) Phosphorylation of Rho-kinase in dissociated cultured cortical neurons. Neurons were treated with DMSO or 10 μM H89 for 30 min and then with or without 10 μM Forskolin and 50 μM IBMX for 30 min. The cell lysates were analyzed using immunoblot analysis with anti-phospho-Rho-kinase (pS1379) Ab (upper panel) or mouse anti-Rho-kinase Ab (lower panel). (E) Phosphorylation of Rho-kinase in the murine striatum. Striatal slices were incised from male C57BL/6 mice at 6–8 weeks old. The slices were treated with or without 100 μM dopamine for 4 min. The slices were mixed with SDS sample buffer and subjected to immunoblot analysis with anti-phospho-Rho-kinase (pS1379) Ab (upper panel) or mouse anti-Rho-kinase Ab (lower panel).

amount according to PKA activation and inhibition. Indeed, we could not find the phosphopeptide containing serine 1379 of Rho-kinase in the enriched fraction by TiO2 column, even ion intensity in FSK/IBMX-treated sample was less than two times higher than control sample. We suppose that the predicted phosphopeptide containing serine 1379 of Rho-kinase (PpSR) would be hard to be detected under our experimental condition, due to the small m/z value. Total peptide analysis is expected to pick up such candidate substrates. We obtained many candidate substrates that were not detected in the phosphopeptide analysis. Thus, enriched phosphopeptide analysis and total peptide analysis can complement each other to improve the detection of phosphorylated proteins.

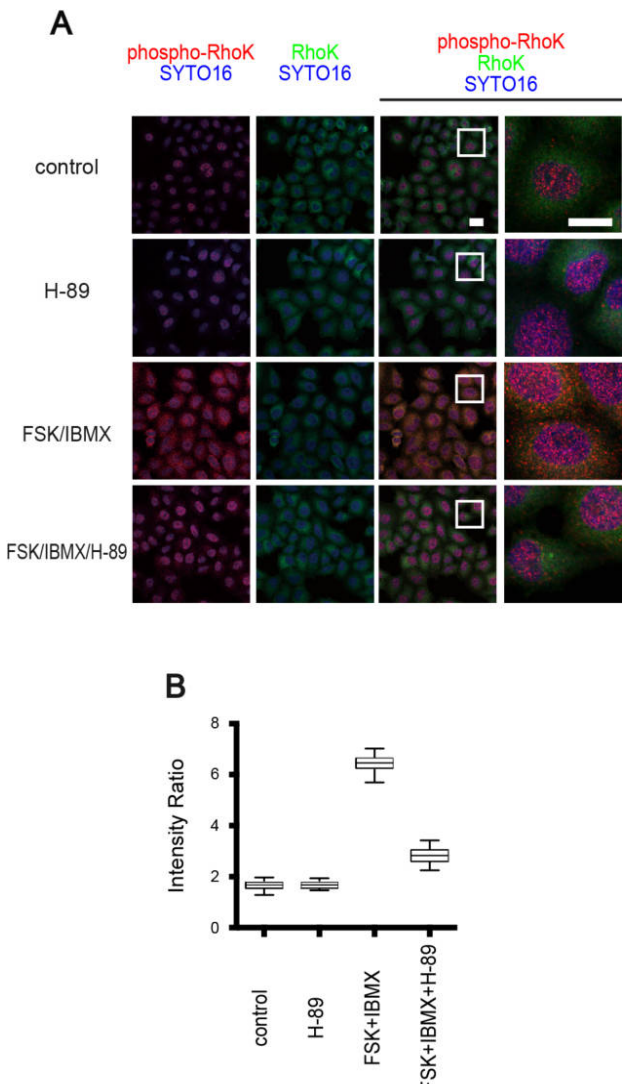

Among the candidate substrates, we found 10 ribosomal proteins in addition to several proteins involved in ribosomal RNA processing, such as BOP1 and Fibrillarin. It has been reported that ribosomal proteins are phosphorylated by PKA *in vitro* (Traugh and Porter, 1976; Wettenhall and Morgan, 1984). In particular, phosphorylation of the 40S ribosomal subunit by PKA inhibits the translation of poly(A,U,G) using a reconstituted protein synthesizing system (Burkhard and Traugh, 1983). PKA might also phosphorylate those ribosomal proteins detected in our assay to regulate protein synthesis.

Several proteins associated with the actin cytoskeleton were also detected. Activation of PKA has long been known to interfere with the RhoA/Rho-kinase signaling pathway. Upon the activation of RhoA by extracellular stimuli, Rho-kinase is activated by RhoA and regulates cellular contractility via the phosphorylation of myosin phosphatase-targeting subunit 1 (MYPT1) and myosin light chain (MLC) (Amano *et al.*, 1996a). It was reported that PKA phosphorylates RhoA at its C-terminus and that treatment of cells with Bt2cAMP results in the translocation of membrane-associated RhoA toward the cytosol (Lang *et al.*, 1996). Phosphorylation of RhoA by PKA *in vitro* also decreases the binding of RhoA to Rho-kinase (Dong *et al.*, 1998). Phosphorylation of MYPT1 by PKA prevents its phosphorylation by Rho-kinase and therefore enhances the activity of myosin phosphatase (Wooldridge *et al.*, 2004). Therefore, PKA signaling has an inhibitory effect on Rho

Fig. 5. Localization of phosphorylated Rho-kinase in HeLa cells. (A) Immunostaining of HeLa cells treated with FSK/IBMX and/or H-89. HeLa cells were treated with/without 15 μM H-89 for 30 min and subsequently with/without 20 μM FSK/100 μM IBMX for 30 min. HeLa cells were fixed in 4% paraformaldehyde for 15 min at room temperature. After washing, the cells were immunostained with mouse anti-Rho-kinase Ab and anti-phospho-Rho-kinase (pS1379) Ab79 Ab. Colors indicate Rho-kinase (green), Rho-kinase pS1379 (red) and SYTO16 (blue). Scale bar, 20 μm. (B) The intensity ratios of Rho-kinase pS1379 to Rho-kinase in the cytosol of HeLa cells. Each intensity ratio represents the signal intensity of phosphorylated Rho-kinase at serine 1379 divided by the signal intensity of total Rho-kinase. The data represent the means±SD of more than three independent experiments. n=30 on each drug condition. *** $p \leq 0.001$ (Tukey's multiple-comparison test). (C) Schematic illustration of PKA signaling associated with Rho signaling at multiple steps. PKA may inhibit Rho-kinase activity by phosphorylating at serine 1379 (red arrows).

signaling (Fig. 5C). Here, we found that PKA phosphorylates Rho-kinase in both HeLa cells and neurons, and we further tried several approaches to determine whether PKA signaling also has an inhibitory effect on Rho-kinase activity. First, we compared the activity of Rho-kinase immunoprecipitated from COS-7 cells treated by FSK/IBMX with that from control cells by an *in vitro* kinase assay but did not detect a significant difference (data not shown). Next, we examined the effect of phosphorylation on the intramolecular association between the catalytic and RB/PH regions of Rho-kinase; a closed configuration suppresses Rho-kinase function but active RhoA is supposed to disrupt this interaction (Amano *et al.*, 1999). GST-Rho-kinase-cat-KD was co-expressed with GFP-Rho-kinase-RB/PH(TT) in COS-7 cells and pulled down with glutathione beads. The amount of co-precipitated GFP-Rho-kinase-RB/PH(TT) was not altered by the mutation of serine 1379 (data not shown). These results suggest that the phosphorylation of Rho-kinase by PKA does not change its basal kinase activity or intramolecular binding. From our immunostaining data, we found that PKA activation increased the intensity of phosphorylated Rho-kinase in the cytosol. The staining with phospho-Rho-kinase antibody displayed dot-like structures, and we could not clarify the structures. We previously examined the intracellular distribution of Rho-kinase (ROCK1 and ROCK2) in various mouse tissues both by light microscopy and electron microscopy (Iizuka *et al.*, 2012). In this report, Rho-kinase (ROCK2) immunoreactivity was sometimes observed as clusters in the cytoplasm in addition to actin cytoskeleton and cell adhesion sites. We confirmed that these clusters were not associated with the cytoskeleton or any organelle, and their function remains unknown. Because serine 1379 resides at the C terminus of Rho-kinase close to the PH domain, phosphorylation by PKA might prevent Rho-kinase from binding to the membrane or actin cytoskeleton, thus translocating Rho-kinase to the cytosol. As a consequence, this phosphorylation might inhibit Rho-kinase activity in the cell (Fig. 5C). During the course of our study, Gerarduzzi *et al.*, reported that PKA phosphorylates Rho-kinase at serine 1379 in synovial fibroblasts downstream of PGE_2 and that expression of non-phosphorylated Rho-kinase mutant at serine 1379 prevents the PGE_2-induced MLC dephosphorylation and cytoskeletal reorganization (Gerarduzzi *et al.*, 2014), which is consistent with our hypothesis.

Although a comparison of the homology between Rho-kinase and ROCK1 shows that they have 92% identity in their kinase domains, the C terminal regions containing the PH domain of Rho-kinase and ROCK1 have only 66% sequence identity (Leung *et al.*, 1996; Nakagawa *et al.*, 1996). Furthermore, the sequence surrounding serine 1379 of Rho-kinase is different from that of ROCK1. It has been reported that the difference in activity between Rho-kinase and ROCK1 originates, in part, from the distinct lipid-binding preferences of their PH domains (Yoneda *et al.*, 2005). Our data show that phosphorylation of Rho-kinase by PKA was detected with anti-phospho-PKA substrate Ab but that ROCK1 was not. Thus, the phosphorylation of Rho-kinase at serine 1379 by PKA could contribute to the differences observed in Rho-kinase and ROCK1 activity. The molecular mechanisms underlying Rho-kinase regulation and the differences between Rho-kinase and ROCK1 remain an issue for future investigation.

Acknowledgments. We thank Drs. Y. Kirii and K. Yoshino (Carna Biosciences) for providing us with recombinant kinase, and Prof. Y. Ishihama (Kyoto University) for technical advice and helpful discussion. We thank Mr. F. Ishidate for help with acquiring and analyzing images. We also thank all the members of Kaibuchi laboratory, especially Drs. K. Kato, K. Kuroda, K. Matsuzawa, M. Kakeno, T. Matsui, for discussion and technical support. We are grateful to Mss. Y. Kanazawa and T. Ishii for technical and secretarial assistance. This research was supported in part by Grant-in-Aid for Scientific Research (S) (20227006), (A) (25251021) and (C) (23590357) from the Ministry of Education, Culture, Sports, Science and Technology of Japan (MEXT). A part of this study is the result of "Bioinformatics for brain sciences" carried out under the Strategic Research Program for Brain Sciences and Grant-in-Aid for Scientific Research on Innovative Areas (Comprehensive Brain Science Network) by MEXT.

References

Amano, M., Ito, M., Kimura, K., Fukata, Y., Chihara, K., Nakano, T., Matsuura, Y., and Kaibuchi, K. 1996a. Phosphorylation and activation of myosin by Rho-associated kinase (Rho-kinase). *J. Biol. Chem.*, **271**: 20246–20249.

Amano, M., Mukai, H., Ono, Y., Chihara, K., Matsui, T., Hamajima, Y., Okawa, K., Iwamatsu, A., and Kaibuchi, K. 1996b. Identification of a putative target for Rho as the serine-threonine kinase protein kinase N. *Science*, **271**: 648–650.

Amano, M., Chihara, K., Nakamura, N., Kaneko, T., Matsuura, Y., and Kaibuchi, K. 1999. The COOH terminus of Rho-kinase negatively regulates rho-kinase activity. *J. Biol. Chem.*, **274**: 32418–32424.

Amano, M., Nakayama, M., and Kaibuchi, K. 2010. Rho-kinase/ROCK: A key regulator of the cytoskeleton and cell polarity. *Cytoskeleton*, **67**: 545–554.

Burkhard, S.J. and Traugh, J.A. 1983. Changes in ribosome function by cAMP-dependent and cAMP-independent phosphorylation of ribosomal protein S6. *J. Biol. Chem.*, **258**: 14003–14008.

Butt, E., Abel, K., Krieger, M., Palm, D., Hoppe, V., Hoppe, J., and Walter, U. 1994. cAMP- and cGMP-dependent protein kinase phosphorylation sites of the focal adhesion vasodilator-stimulated phosphoprotein (VASP) in vitro and in intact human platelets. *J. Biol. Chem.*, **269**: 14509–14517.

Chuang, H.H., Yang, C.H., Tsay, Y.G., Hsu, C.Y., Tseng, L.M., Chang, Z.F., and Lee, H.H. 2012. ROCKII Ser1366 phosphorylation reflects the activation status. *Biochem. J.*, **443**: 145–151.

Cox, J. and Mann, M. 2008. MaxQuant enables high peptide identification rates, individualized p.p.b.-range mass accuracies and proteome-wide protein quantification. *Nat. Biotechnol.*, **26**: 1367–1372.

Dong, J.M., Leung, T., Manser, E., and Lim, L. 1998. cAMP-induced morphological changes are counteracted by the activated RhoA small GTPase and the Rho kinase ROKalpha. *J. Biol. Chem.*, **273**: 22554–22562.

Engh, R.A., Girod, A., Kinzel, V., Huber, R., and Bossemeyer, D. 1996. Crystal Structures of Catalytic Subunit of cAMP-dependent Protein Kinase in Complex with Isoquinolinesulfonyl Protein Kinase Inhibitors

H7, H8, and H89. STRUCTURAL IMPLICATIONS FOR SELECTIVITY. *J. Biol. Chem.*, **271**: 26157–26164.

Gerarduzzi, C., He, Q., Antoniou, J., and Di Battista, J.A. 2014. Prostaglandin E2 -Dependent Blockade of Actomyosin and Stress Fibre Formation Is Mediated Through S1379 Phosphorylation of ROCK2. *J. Cell. Biochem.*, **115**: 1516–1527.

Ghanouni, P., Gryczynski, Z., Steenhuis, J.J., Lee, T.W., Farrens, D.L., Lakowicz, J.R., and Kobilka, B.K. 2001. Functionally different agonists induce distinct conformations in the G protein coupling domain of the beta 2 adrenergic receptor. *J. Biol. Chem.*, **276**: 24433–24436.

Gonzalez, G.A. and Montminy, M.R. 1989. Cyclic AMP stimulates somatostatin gene transcription by phosphorylation of CREB at serine 133. *Cell*, **59**: 675–680.

Goslin, K. and Banker, G. 1989. Experimental observations on the development of polarity by hippocampal neurons in culture. *J. Cell Biol.*, **108**: 1507–1516.

Granot, J., Mildvan, A.S., Hiyama, K., Kondo, H., and Kaiser, E.T. 1980. Magnetic resonance studies of the effect of the regulatory subunit on metal and substrate binding to the catalytic subunit of bovine heart protein kinase. *J. Biol. Chem.*, **255**: 4569–4573.

Holz, G.G.t., Rane, S.G., and Dunlap, K. 1986. GTP-binding proteins mediate transmitter inhibition of voltage-dependent calcium channels. *Nature*, **319**: 670–672.

Iizuka, M., Kimura, K., Wang, S., Kato, K., Amano, M., Kaibuchi, K., and Mizoguchi, A. 2012. Distinct distribution and localization of Rho-kinase in mouse epithelial, muscle and neural tissues. *Cell Struct. Funct.*, **37**: 155–175.

Inagaki, N., Chihara, K., Arimura, N., Menager, C., Kawano, Y., Matsuo, N., Nishimura, T., Amano, M., and Kaibuchi, K. 2001. CRMP-2 induces axons in cultured hippocampal neurons. *Nat. Neurosci.*, **4**: 781–782.

Kemp, B.E., Bylund, D.B., Huang, T.S., and Krebs, E.G. 1975. Substrate specificity of the cyclic AMP-dependent protein kinase. *Proc. Natl. Acad. Sci. USA*, **72**: 3448–3452.

Kemp, B.E., Graves, D.J., Benjamini, E., and Krebs, E.G. 1977. Role of multiple basic residues in determining the substrate specificity of cyclic AMP-dependent protein kinase. *J. Biol. Chem.*, **252**: 4888–4894.

Lang, P., Gesbert, F., Delespine-Carmagnat, M., Stancou, R., Pouchelet, M., and Bertoglio, J. 1996. Protein kinase A phosphorylation of RhoA mediates the morphological and functional effects of cyclic AMP in cytotoxic lymphocytes. *EMBO J.*, **15**: 510–519.

Le Peuch, C.J., Haiech, J., and Demaille, J.G. 1979. Concerted regulation of cardiac sarcoplasmic reticulum calcium transport by cyclic adenosine monophosphate dependent and calcium--calmodulin-dependent phosphorylations. *Biochemistry*, **18**: 5150–5157.

Leung, T., Chen, X.Q., Manser, E., and Lim, L. 1996. The p160 RhoA-binding kinase ROK alpha is a member of a kinase family and is involved in the reorganization of the cytoskeleton. *Mol. Cell. Biol.*, **16**: 5313–5327.

Mann, M., Ong, S.E., Gronborg, M., Steen, H., Jensen, O.N., and Pandey, A. 2002. Analysis of protein phosphorylation using mass spectrometry: deciphering the phosphoproteome. *Trends Biotechnol.*, **20**: 261–268.

Moritz, A., Li, Y., Guo, A., Villen, J., Wang, Y., MacNeill, J., Kornhauser, J., Sprott, K., Zhou, J., Possemato, A., Ren, J.M., Hornbeck, P., Cantley, L.C., Gygi, S.P., Rush, J., and Comb, M.J. 2010. Akt-RSK-S6 kinase signaling networks activated by oncogenic receptor tyrosine kinases. *Sci. Signal.*, **3**: ra64.

Nakagawa, O., Fujisawa, K., Ishizaki, T., Saito, Y., Nakao, K., and Narumiya, S. 1996. ROCK-I and ROCK-II, two isoforms of Rho-associated coiled-coil forming protein serine/threonine kinase in mice. *FEBS Lett.*, **392**: 189–193.

Nishi, A., Snyder, G.L., and Greengard, P. 1997. Bidirectional regulation of DARPP-32 phosphorylation by dopamine. *J. Neurosci.*, **17**: 8147–8155.

Nishioka, T., Nakayama, M., Amano, M., and Kaibuchi, K. 2012. Proteomic screening for Rho-kinase substrates by combining kinase and phosphatase inhibitors with 14-3-3zeta affinity chromatography. *Cell Struct. Funct.*, **37**: 39–48.

Peng, J., Elias, J.E., Thoreen, C.C., Licklider, L.J., and Gygi, S.P. 2003. Evaluation of multidimensional chromatography coupled with tandem mass spectrometry (LC/LC-MS/MS) for large-scale protein analysis: the yeast proteome. *J. Proteome Res.*, **2**: 43–50.

Pohl, S.L., Krans, H.M., Kozyreff, V., Birnbaumer, L., and Rodbell, M. 1971. The glucagon-sensitive adenyl cyclase system in plasma membranes of rat liver. VI. Evidence for a role of membrane lipids. *J. Biol. Chem.*, **246**: 4447–4454.

Riento, K. and Ridley, A.J. 2003. Rocks: multifunctional kinases in cell behaviour. *Nat. Rev. Mol. Cell Biol.*, **4**: 446–456.

Self, D.W., Genova, L.M., Hope, B.T., Barnhart, W.J., Spencer, J.J., and Nestler, E.J. 1998. Involvement of cAMP-dependent protein kinase in the nucleus accumbens in cocaine self-administration and relapse of cocaine-seeking behavior. *J. Neurosci.*, **18**: 1848–1859.

Tesmer, J.J., Sunahara, R.K., Gilman, A.G., and Sprang, S.R. 1997. Crystal structure of the catalytic domains of adenylyl cyclase in a complex with Gsalpha.GTPgammaS. *Science*, **278**: 1907–1916.

Traugh, J.A. and Porter, G.G. 1976. A comparison of ribosomal proteins from rabbit reticulocytes phosphorylated in situ and in vitro. *Biochemistry*, **15**: 610–616.

Walsh, D.A., Perkins, J.P., and Krebs, E.G. 1968. An adenosine 3',5'-monophosphate-dependant protein kinase from rabbit skeletal muscle. *J. Biol. Chem.*, **243**: 3763–3765.

Walsh, D.A. and Van Patten, S.M. 1994. Multiple pathway signal transduction by the cAMP-dependent protein kinase. *FASEB J.*, **8**: 1227–1236.

Wettenhall, R.E. and Morgan, F.J. 1984. Phosphorylation of hepatic ribosomal protein S6 on 80 and 40 S ribosomes. Primary structure of S6 in the region of the major phosphorylation sites for cAMP-dependent protein kinases. *J. Biol. Chem.*, **259**: 2084–2091.

Wooldridge, A.A., MacDonald, J.A., Erdodi, F., Ma, C., Borman, M.A., Hartshorne, D.J., and Haystead, T.A. 2004. Smooth muscle phosphatase is regulated in vivo by exclusion of phosphorylation of threonine 696 of MYPT1 by phosphorylation of Serine 695 in response to cyclic nucleotides. *J. Biol. Chem.*, **279**: 34496–34504.

Yamamoto, K.K., Gonzalez, G.A., Biggs, W.H., 3rd, and Montminy, M.R. 1988. Phosphorylation-induced binding and transcriptional efficacy of nuclear factor CREB. *Nature*, **334**: 494–498.

Yoneda, A., Multhaupt, H.A., and Couchman, J.R. 2005. The Rho kinases I and II regulate different aspects of myosin II activity. *J. Cell Biol.*, **170**: 443–453.

Zhang, H., Zha, X., Tan, Y., Hornbeck, P.V., Mastrangelo, A.J., Alessi, D.R., Polakiewicz, R.D., and Comb, M.J. 2002. Phosphoprotein analysis using antibodies broadly reactive against phosphorylated motifs. *J. Biol. Chem.*, **277**: 39379–39387.

(Received for publication, September 27, 2014, accepted, November 10, 2014 and published online, November 14, 2014)